

32 applications related to infotainment systems will also lead to channel contention and spectrum
33 deficiency. In view of the stringent QoS requirements on DSRC spectrum, it is not sufficient
34 for all applications to depend only on the 5.9-GHz DSRC spectrum. There is a dramatic increase in the
35 demand for frequency resources to satisfy their communication requirements.

36 To relieve the bottleneck problem of spectrum deficiency, cognitive radio (CR) [1], [2] has
37 increasingly been presented as a potential technique being capable of accessing licensed but unoccupied
38 frequency bands only without causing any unacceptable interference to licensed users (or primary
39 users, PUs). Cognitive radio has become one of the most breathtaking technologies to improve the
40 spectrum efficiency effectively for the past couple of decades. In addition to a better remedy for
41 frequency scarcity issue, cognitive radio is appropriate for vehicular environments, since their unique
42 characteristics make it much better to achieve the spatial and temporal reuse of the empty frequency
43 bands of PUs compared to other traditional cognitive networks [3], [4]. To efficiently reuse the
44 spectrum holes with minimum interference to PUs, the CR-enabled vehicles, which can be called
45 secondary vehicular users (SVUs), need to reliably make a decision about the existence of PUs. And
46 they must immediately vacate the radio channels as soon as PUs are detected. Consequently, spectrum
47 sensing constitutes the key component of cognitive vehicular networks (CVNs) [7].

48 Spectrum sensing [5] is a wealthily investigated subject, but is more concentrated in traditional
49 CR networks. Among them, cooperative sensing [6] has already attracted strong research interest as it
50 can take further advantage of both spatial and temporal diversity, and thereby garner better sensing
51 accuracy and efficiency in the face of fading. However, these existing spectrum sensing techniques can
52 not be directly applicable to vehicular networks. And it's all because we have to give an account of the
53 idiosyncrasies of vehicular networks such as high mobility while designing sensing schemes for CVNs
54 [3], [8]. For instance, rapid movement of vehicles makes the availability of spectrum holes dynamically
55 change since a vehicle may enter or leave a region interfered by a particular PU at different locations
56 along the road. In this regard, it is considerable for SVUs to detect PU activities in the fastest possible
57 way. Additionally, the vehicles' motion are restricted and predictable due to the fixed road topology.
58 In consequence, each vehicle may be glad to know in advance the spectrum opportunities to better
59 utilize them for transmission on its track. Further, high speeds and the environmental clutter can affect
60 the received signal due to Doppler effect, fading and shadowing. These factors will have immediate
61 impacts on spectrum sensing of CVNs.

62 Spectrum sensing in dynamic vehicular environments have been researched in some preliminary
63 works [4], [9], [10], [11], [12]. The authors in [4] proposed a novel adaptive sensing coordinated
64 mechanism, in which the central node merely assist and coordinate the SVUs to better acquire the
65 availability of spectrum holes instead of completely controlling the sensing and access. The authors
66 in [9] studied the detection performance of spectrum sensing under the shadowing and multi-path
67 composite fading channel in vehicular environments. The authors in [10] presented an asynchronous
68 collaborative sensing framework in which the tagged vehicle collects energy measurements labeled
69 with time and location information from collaborative SVUs and assigns weights based on their storing
70 time and location. The authors in [11] proposed a distributed collaborative sensing scheme based
71 on adaptive decision threshold for sensing and voting scheme for connected vehicles. An integrated
72 overview of spectrum sensing in cognitive vehicular environments can be discovered in [12]. None
73 of these previous researches considered the effect of temporal correlation due to vehicle motion and
74 multi-path propagation in a mobile vehicular environment. Moreover, the reporting channels between
75 SVUs and the fusion center (FC) were assumed to be ideal.

76 In this paper, our attention is centered on large-scale fixed PUs detection in an infrastructure-based
77 CVN based on mutual benefit and acquiring a win-win situation by allowing the back vehicles utilize
78 the spectrum availability information after front vehicles sensed. Each SVU periodically performs
79 sensing and reports its sensing information via the dedicated reporting channel to the nearby FC.
80 The FC fuses the received information to make a global decision for the current cell. At this moment,
81 some vehicles taking part in cooperative sensing may have left this cell. We investigate the sensing

82 performance using hard fusion [13]. Although soft fusion can gather improved performance than hard
83 fusion, the burden of reporting overhead impedes its applicability [14]. Our research in this paper
84 distinct from the previous works in two respects: 1) look at the effect of fading correlation and their
85 severity on spectrum sensing performance under temporally correlated Rayleigh sensing channel;
86 and 2) make clear how dramatically the reporting channel conditions could influence the reliability
87 of a local/global decision, when made by the FC. For local and cooperative sensing, we evaluate the
88 sensing performances through theoretical analysis or Monte Carlo simulation. Our results shows that
89 poor channel conditions harms the detection performance. However, amazingly, we will demonstrate
90 that the fast time-varying characteristic of sensing channels can give us an opportunity to obtain
91 temporal diversity provided that a proper sensing technique is adopted.

92 The rest of the paper is organized as follows. In Section 2, we describe system model and
93 assumptions on spectrum sensing in vehicular environments. In Section 3, the local sensing
94 performance over correlated Rayleigh fading is analyzed. In Section 4, we consider the cooperative
95 sensing performance with fading reporting channels. This is followed by the numerical and simulated
96 results in Section 5. Lastly, we summarize the conclusions in Section 6.

97 Throughout this paper on detection performance, we will declare the local probabilities of false
98 alarm, miss detection, and detection as P_f , P_m , and P_d , respectively, whereas their equivalent local
99 probabilities will be represented by P_F , P_M , and P_D and their global probabilities Q_f , Q_m , and Q_d
100 for hard fusion.

101 2. System Model and Problem Formulation

102 In this section, we briefly introduce the network model, the channel model, the sensing model,
103 and the assumptions made in the CVNs under consideration.

104 2.1. Network Model

105 We consider a vehicular network in multi-lane highway scenarios in which licensed and cognitive
106 users coexisting peacefully within the same geospatial region and share multiple frequency channels,
107 like the one depicted in Fig.1. We suppose a large-scale fixed licensed user, such as licensed DTV
108 spectrum holders. The cognitive network is an infrastructure-aided network, in which each cell is
109 composed of a fusion center and a number of associated SVUs. The FC coordinates SVUs collaborative
110 sensing and their access to a vacant PU channel. Each SVU periodically performs sensing and reports
111 its sensing information via the dedicated reporting channel to the nearby FC. According to the received
112 local sensing results, the FC arrives at a global decision for the current cell. At this moment, some
113 vehicles engaged in cooperative sensing may have left this cell. Hence, the FC diffuses the global
114 decision to the next passing SVUs. We postulate that the vehicles move independently from any other,
115 and thus, the sensing channels between PU and SVUs are all independent of one another.

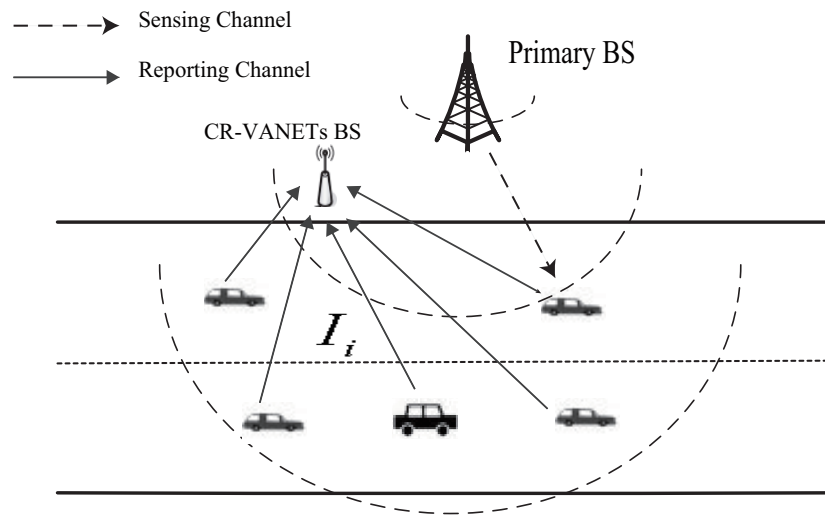


Figure 1. An illustrative example of cooperative sensing operation for cognitive vehicular networks. There are a PU, cooperative SVUs, and a CR-BS over wireless sensing/reporting channels.

116 2.2. Channel Model

In the above scenario, we consider the wireless channels, which have no correlation in space but are temporally correlated following the Jakes' model of land mobile fading channel (Table 2.1 in [15]). Let $\rho(\tau)$ denotes the correlation coefficient between two samples separating τ time interval, which satisfies

$$\rho(\tau) = \mathcal{J}_0(2\pi F_d T_s \tau) \quad (1)$$

117 where $\mathcal{J}_v(\cdot)$ is defined by the v th-order Bessel function of the first kind, and $F_d T_s$ represents normalized
 118 Doppler shift, $F_d T_s = \frac{f_c v}{c} T_s$, which may relate to a vehicle speed v , a carrier frequency f_c and the
 119 sampling interval T_s .

120 The correlation specialities of the fading progress depend only on $F_d T_s$, as illustrated in fig. 2.
 121 Based on the different $F_d T_s$, we can employ a suitable model, which is convenient to analyze the fading
 122 characteristics of sensing channel. For instance, three different models, \mathcal{M}_1 , \mathcal{M}_2 and \mathcal{M}_3 , are given as
 123 follows, respectively

124 \mathcal{M}_1 : When $F_d T_s$ is relatively smaller (< 0.001), the channel process is nearly time-invariant.

125 \mathcal{M}_2 : When $F_d T_s$ is small (< 0.02), the channel process is correlated ("slow" fading).

126 \mathcal{M}_3 : For larger values of $F_d T_s$ (> 0.03), the channel process are almost independent time-varying
 127 ("fast" fading).

128 Note that \mathcal{M}_1 and \mathcal{M}_3 are two extreme cases of temporally correlated Rayleigh fading channel.

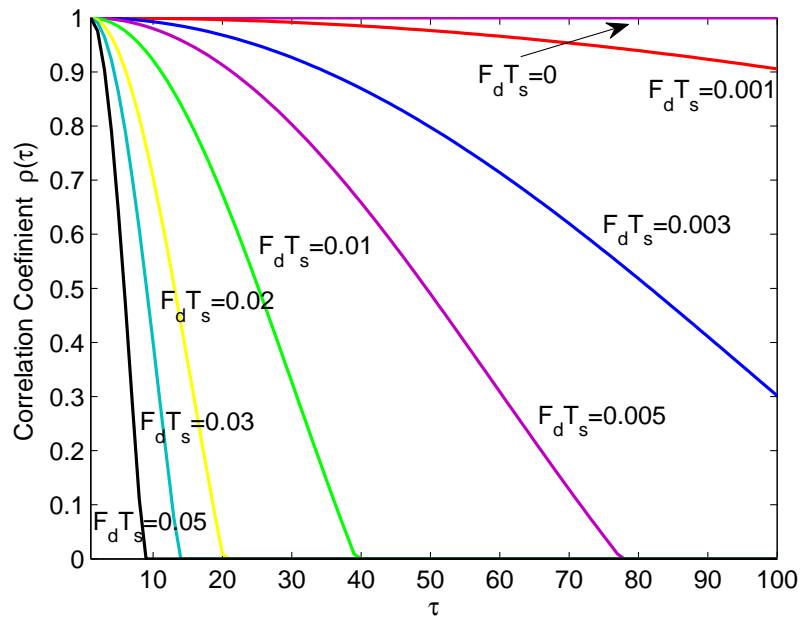


Figure 2. The correlation coefficient for various $F_d T_s$.

129 2.3. Sensing Model

Spectrum sensing is a binary hypothesis detection issue, with the null (\mathcal{H}_0) and alternative (\mathcal{H}_1) hypotheses associated to the presence and absence of PU in a given frequency band, respectively. We consider a cognitive vehicular network consisting of N collaborative SVUs. Assume L sampling observations can be used within a sensing interval. Under both hypotheses, the received observation by SUV i at the k th time instant can be expressed as, respectively

$$x_i(k) = \begin{cases} n_i(k) & \mathcal{H}_0 \\ h_i(k)s(k) + n_i(k) & \mathcal{H}_1 \end{cases} \quad (2)$$

130 where, $s(k)$ is the baseband-equivalent signal transmitted by the PU, $x_i(k)$ denotes the received
 131 signal by SVU i , $h_i(k)$ denotes the sensing channel gain with $E[|h_i(k)|^2] = 1$, and $n_i(k)$ denotes
 132 white and circularly symmetric complex Gaussian (CSCG) noise with mean zero and variance σ_n^2 , i.e.,
 133 $n_i(k) \sim \mathcal{CN}(0, \sigma_n^2)$. It's assumed that $s(k)$, $h_i(k)$ and $n_i(k)$ are independent of each other, which is
 134 reasonable from a practical situation.

To reduce the complexity and reporting channel overhead, each SVU employs a mapping rule to its observations, to produce a quantized information denoted by $q(x_i)$. In this paper, we suppose each SUV makes a binary decision $u_i = q(x_i) \in \{+1, -1\}$ with probabilities of false-alarm and mis-detection P_{fi} and P_{mi} . These decisions are then reported to the FC via a fading reporting channel or link, bit error may happen, which further affects the sensing performance at the FC. We will model the reporting channel as a Rayleigh fading channel. The received observation at the FC from the i th node can be described as

$$z_i = g_i u_i + w_i \quad (3)$$

135 where g_i is the fading gain of reporting channel and w_i is a zero-mean Gaussian random variable
 136 with variance δ_i^2 , i.e., $w_i \sim \mathcal{N}(0, \delta_i^2)$. Once the noisy observation $\{z_i; i = 1, 2, \dots, N\}$ is received and
 137 decoded, the FC makes a global decision on which hypothesis is more likely to be true.

138 In the ordinary sense, an optimal fusion rule for hard combination is behaved in the form of
 139 a counting rule [16]. This argument proves to be true even when those decisions are received via
 140 unreliable communication channels, provided that the channels are also independent and identical
 141 distribution (IID). In the latter of this paper, we focus on energy detection for spectrum sensing and
 142 look at the detection performance of the counting rule in Rayleigh fading channels.

143 3. Local Sensing with Energy Detection

144 For local sensing, we consider energy detection (ED) instead of other sensing techniques, such as
 145 the cyclostationary feature detection which takes high computational complexity and much longer
 146 sensing time because it exploits a specific signature of the PU signal. Energy detection [17], [18] is
 147 the most practical and robust detection method because it merely estimates the signal energy on
 148 the considered band and produces very good performance without any *priori* information about PU
 149 signals, as illustrated in fig. 3. Furthermore, Energy detection is a viable choice for vehicular networks
 150 on account of its high mobile environment and low latency tolerant.

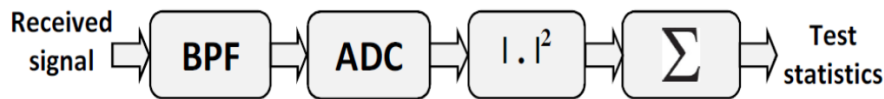


Figure 3. Energy detector model.

Consequently, the local test statistic of the energy detector at the i th SUV, denoted by e_i , is basically an estimate of received signal energy which is represented as:

$$e_i = \sum_{k=0}^{L-1} |x_i(k)|^2 \quad (4)$$

Let λ denotes the local decision threshold and u_i denote the local decision of the i th SVU, the decision rule used by energy detector at each SVU can be expressed as

$$u_i = \begin{cases} +1 & \text{if } e_i \geq \lambda \\ -1 & \text{if } e_i < \lambda \end{cases} \quad (5)$$

151 This means that when e_i is greater than or equal to λ , SVU i makes its individual decision $u_i = +1$
 152 which tells PU signal is detected (\mathcal{H}_1); otherwise, it makes a decision $u_i = -1$ which declares that PU
 153 signal is not detected (\mathcal{H}_0).

For a high number of sensing observations L , on the basis of the Central Limit Theorem (CLT), the local test statistic e_i given by (3) can be well modeled by a normal or Gaussian distribution under either \mathcal{H}_0 or \mathcal{H}_1 [17]. Accordingly, the probability density function (PDF) of e_i at individual SVU can be compactly characterized by

$$e_i \sim \begin{cases} \mathcal{N}(L\sigma_n^2, L\sigma_n^4) & \mathcal{H}_0 \\ \mathcal{N}[(L + \eta_i)\sigma_n^2, (L + 2\eta_i)\sigma_n^4] & \mathcal{H}_1 \end{cases} \quad (6)$$

where

$$\eta_i = \sum_{k=0}^{L-1} |h_i(k)|^2 \frac{E_s}{L\sigma_n^2} \quad (7)$$

154 represents the instantaneous signal-to-noise ratio (SNR) experienced by the i -th SVU within the current
 155 sensing period. It is straightforward to see that η_i varies from (sensing) period to period, since it

156 generally hinges upon the fading characteristics of the wireless channel. And $E_s = \sum_{k=0}^{L-1} |s(k)|^2$ denotes
 157 the transmitted signal energy by the primary user over a sensing interval of L sampling observations.

In the above discussed case, the probabilities of false alarm, miss detection and detection for local sensing at the i -th SVU can be represented by the following formulas, respectively

$$P_{fi}(\lambda) = P(e_i \geq \lambda | \mathcal{H}_0) = \mathcal{Q}\left(\frac{\lambda - L\sigma_n^2}{\sqrt{L}\sigma_n^2}\right) \quad (8)$$

$$P_{di}(\lambda) = P(e_i \geq \lambda | \mathcal{H}_1) = \mathcal{Q}\left(\frac{\lambda - (L + \eta_i)\sigma_n^2}{\sqrt{L + 2\eta_i}\sigma_n^2}\right) \quad (9)$$

$$P_{mi}(\lambda) = P(e_i < \lambda | \mathcal{H}_1) = \mathcal{Q}\left(\frac{(L + \eta_i)\sigma_n^2 - \lambda}{\sqrt{L + 2\eta_i}\sigma_n^2}\right) \quad (10)$$

158 where $\mathcal{Q}(x)$ is defined by the complementary cumulative distribution function of the standard
 159 Gaussian, i.e., $\mathcal{Q}(x) = \frac{1}{\sqrt{2\pi}} \int_x^\infty \exp(-\frac{t^2}{2}) dt$.

160 It's apparent that, P_{fi} in (8) is independent of received SNR because P_{fi} is considered for the
 161 hypothesis of no PU signal transmission. On the other hand, P_{mi} in (10) is a conditional probability
 162 depending on instantaneous received SNR η_i . In this circumstance, the average P_m can be calculated
 163 by integrating the conditional P_{mi} over the SNR fading distribution [17], or quantify the quality of each
 164 channel by its corresponding average received SNR.

From (8) and (10), we also see that, λ can be analytically set to maintain the desired P_f if P_f is designated as the constraint of the detection problem. Then, we obtain P_{mi} related to the desired P_f as follows

$$P_{mi}(\eta_i) = \mathcal{Q}\left(\frac{\eta_i - \sqrt{L}\mathcal{Q}^{-1}(P_f)}{\sqrt{L + 2\eta_i}}\right) \quad (11)$$

165 where $\mathcal{Q}^{-1}(x)$ is defined by the inverse function of $\mathcal{Q}(x)$.

Next, we first consider the case of \mathcal{M}_1 , in which the vehicles move more slowly, $F_d T_s$ is small (< 0.001). And thus, the channel gain $h_i(k)$ remain virtually unchanged during the sensing interval, i.e., $h_i(k) = h_i$ for $k = 1, 2, \dots, L$. Thus, η_i given by (7) can be rewritten as:

$$\eta_i = |h_i|^2 \frac{E_s}{\sigma_n^2} = |h_i|^2 \eta_s \quad (12)$$

166 where $\eta_s = \frac{E_s}{\sigma_n^2}$ is the local average SNR measured at the secondary receiver. It is thus note-worthy that
 167 the local average SNR is L times more than the average SNR measured at the energy detector output,
 168 which can be expressed as $\eta_0 = \frac{E_s}{L\sigma_n^2}$.

Under Rayleigh fading, the instantaneous SNR η_i can be viewed as exponentially distributed

$$f_{\eta_i}(\eta_i) = \frac{1}{\eta_s} e^{-\eta_i/\eta_s} \quad (13)$$

For ease of calculation, we make the following approximation for equation (11) as

$$P_{mi}(\eta_i) \approx \mathcal{Q}\left(\frac{\eta_i - \sqrt{L}\mathcal{Q}^{-1}(P_f)}{\sqrt{L + 2\eta_s}}\right) \quad (14)$$

In what follows we shall define, for the sake of conciseness

$$A = \frac{1}{\sqrt{L + 2\eta_s}}, B = \frac{\sqrt{L}Q^{-1}(P_f)}{\sqrt{L + 2\eta_s}}$$

then

$$P_{mi}(\eta_i) \approx Q(A\eta_i - B) \quad (15)$$

Consequently, the average P_m in the case of \mathcal{M}_1 , \bar{P}_m , can be calculated by integrating (15) over (13) and making the change of variable $x = A\eta - B$ yielding

$$\begin{aligned} \bar{P}_m &= \int_0^\infty P_m(\eta_i) f_{\eta_i}(\eta_i) d\eta_i \\ &\approx \frac{1}{\eta_s} \int_0^\infty Q(A\eta_i - B) e^{-\eta_i/\eta_s} d\eta_i \\ &= \frac{1}{A\eta_s} \int_{-B}^\infty Q(x) e^{-\frac{x+B}{A\eta_s}} dx \end{aligned} \quad (16)$$

By capitalizing on the integrating characters of Q -function [19], and after some simplification, we can derive the following formula for \bar{P}_m

$$\bar{P}_m \approx Q(-B) - e^{-\frac{B}{A\eta_s}} e^{\frac{1}{2A^2\eta_s^2}} Q\left(\frac{1}{A\eta_s} - B\right) \quad (17)$$

169 In the case of \mathcal{M}_2 , in order to obtain \bar{P}_m in closed form, it desirable to obtain the PDF of η_i given
170 in (7). Unfortunately, So far as is known, there is no closed-form expression available for such a
171 distribution. Therefore, it is computationally infeasible to obtain a closed-form expression for \bar{P}_m in
172 the present of temporal fading correlation. Instead of deriving a closed-form for \bar{P}_m , we estimate \bar{P}_m
173 through a Monte Carlo simulation.

174 Highly mobility of vehicles lead to an increase in Doppler shift $F_d T_s$, and thereby resulting in
175 degraded correlation among sampling observations. In the case of \mathcal{M}_3 , the sampling observations of
176 the fading channel $\{h_i(k)\}$ are completely independent of each other, η_i given by (7) can be reduced to
177 the following equation

$$\eta_i = \frac{E_s}{\sigma_n^2} \quad (18)$$

178 It is plain to see that η_i is independent of instantaneous fading statistics. Thus, the \bar{P}_m in this case
179 can be computed directly by (10) and (18).

180 4. Cooperative Sensing with Counting Rule

181 The concept of cooperative spectrum sensing is to utilize multiple SVUs at different locations and
182 fuse their independent sensing messages into one unified decision inferring the presence or absence of
183 the PU. In this section, we will ponder this approach based on hard fusion, and also look at the impact
184 of the reporting channel fading to the global detection performance.

185 4.1. Equivalent Local Probability of False Alarm and Miss Detection

In consideration of the unreliable characteristic of the reporting channels, let us determine its effect on the reliability of the decision made by the FC. Let v_i denote the decoded version of z_i for the i th SVU at the FC, the decoded rule can be expressed as

$$v_i = \begin{cases} 1 & \text{if } z_i \geq 0 \\ 0 & \text{if } z_i < 0 \end{cases} \quad (19)$$

And, more remarkable, under the hypothesis \mathcal{H}_j ($j = 0, 1$)

$$\begin{aligned} E[v_i | \mathcal{H}_j] &= P(v_i = 1 | \mathcal{H}_j) \times 1 + P(v_i = 0 | \mathcal{H}_j) \times 0 \\ &= P(z_i \geq 0 | \mathcal{H}_j) \end{aligned} \quad (20)$$

$$\begin{aligned} D[v_i | \mathcal{H}_j] &= E[v_i^2 | \mathcal{H}_j] - E[v_i | \mathcal{H}_j]^2 \\ &= P(z_i \geq 0 | \mathcal{H}_j) - (P(z_i \geq 0 | \mathcal{H}_j))^2 \end{aligned} \quad (21)$$

186 where $E[x]$, $D[x]$ denotes the expectation and variance operator with respect to x .

187 As can be seen from (20) and (21), the expectation and variance of received decision v_i are directly
188 depend on the probability $P(z_i \geq 0 | \mathcal{H}_j)$, which can also be referred to the equivalent probability
189 of false-alarm and mis-detection of local sensing. For notational convenience, let us denote this
190 probability by P_{Fi} and P_{Di} under both hypothesis. In order to capture the statistical properties of v_i ,
191 we first need to obtain the probabilities $P_{Fi} = f(z_i \geq 0 | \mathcal{H}_1)$ and $P_{Di} = f(z_i \geq 0 | \mathcal{H}_0)$.

Clearly, under the hypothesis \mathcal{H}_0 (\mathcal{H}_1), u_i obeys the following distribution with the parameter of P_{fi} (P_{di}).

$$\begin{aligned} P(u_i | \mathcal{H}_0) &= \begin{cases} P_{fi} & u_i = +1 \\ 1 - P_{fi} & u_i = -1 \end{cases} \\ P(u_i | \mathcal{H}_1) &= \begin{cases} 1 - P_{mi} & u_i = +1 \\ P_{mi} & u_i = -1 \end{cases} \end{aligned}$$

Then, under the hypothesis \mathcal{H}_j , the equivalent probability of false alarm and miss detection can be written as:

$$\begin{aligned} P_{Fi} = f(z_i \geq 0 | \mathcal{H}_0) &= \sum_{u_i \in \{+1, -1\}} f(z_i \geq 0 | u_i) P(u_i | \mathcal{H}_0) \\ &= f(z_i \geq 0 | u_i = +1) P_{fi} + f(z_i \geq 0 | u_i = -1) (1 - P_{fi}) \end{aligned} \quad (22)$$

$$\begin{aligned} P_{Di} = f(z_i \geq 0 | \mathcal{H}_1) &= \sum_{u_i \in \{+1, -1\}} f(z_i \geq 0 | u_i) P(u_i | \mathcal{H}_1) \\ &= f(z_i \geq 0 | u_i = +1) P_{di} + f(z_i \geq 0 | u_i = -1) (1 - P_{di}) \end{aligned} \quad (23)$$

Without loss of generality, suppose that the reporting channels between SVUs and FC is also Rayleigh fading channel draw from CSCG distribution $\mathcal{CN}(0, 2)$. In the other words, the PDF of the channel gain g_i can be represented as

$$f(g_i) = \begin{cases} g_i \exp\left(-\frac{g_i^2}{2}\right) & g_i \geq 0 \\ 0 & g_i < 0 \end{cases} \quad (24)$$

On the basis of the fact that $y_i = g_i u_i$, $z_i = y_i + w_i$ and w_i is a zero-mean Gaussian variable with variance δ_i^2 , we can easily get

$$f(y_i | u_i) = \begin{cases} u_i y_i \exp\left(-\frac{y_i^2}{2}\right) & y_i \geq 0 \\ 0 & y_i < 0 \end{cases} \quad (25)$$

$$f(z_i | y_i) = \frac{1}{\sqrt{2\pi}\delta_i} \exp\left(-\frac{(z_i - y_i)^2}{2\delta_i^2}\right) \quad (26)$$

Further still, according to this fact that $f(z_i | y_i, u_i) = f(z_i | y_i)$, which is stemmed from the fact that $(h_i, u_i) \rightarrow y_i \rightarrow z_i$ is a Markov chain, we can safely come to the following result

$$\begin{aligned} f(z_i | u_i) &= \frac{f(z_i, u_i)}{p(u_i)} = \frac{\int f(z_i | y_i, u_i) f(y_i | u_i) p(u_i) dy_i}{p(u_i)} \\ &= \int f(z_i | y_i) f(y_i | u_i) dy_i \end{aligned} \quad (27)$$

Then, substituting (25) and (26) into (27), we can obtain the conditional PDF of the received observation z_i , given the local decision $u_i = +1$, as

$$\begin{aligned} f(z_i | u_i = +1) &= \int_0^\infty \frac{1}{\sqrt{2\pi}\delta_i} \exp\left(-\frac{(z_i - y_i)^2}{2\delta_i^2}\right) y_i \exp\left(-\frac{y_i^2}{2}\right) dy_i \\ &= \frac{1}{\sqrt{2\pi}\delta_i} \exp\left(-\frac{z_i^2}{2(1+\delta_i^2)}\right) \int_0^\infty y_i \exp\left(-\frac{(y_i - \frac{z_i}{1+\delta_i^2})^2}{\frac{2\delta_i^2}{1+\delta_i^2}}\right) dy_i \end{aligned} \quad (28)$$

More specifically performing a change of variable $t = y_i - \frac{z_i}{1+\delta_i^2}$ and making the best of the integral properties of \mathcal{Q} -function, we can obtain

$$f(z_i | u_i = +1) = \frac{C^2 \delta_i^3}{\sqrt{2\pi}} \exp\left(-\frac{z_i^2}{2\delta_i^2}\right) \left[1 + \sqrt{2\pi} C z_i \exp\left(\frac{C^2 z_i^2}{2}\right) \mathcal{Q}(-C z_i)\right] \quad (29)$$

192 where $C = \frac{1}{\delta_i \sqrt{1+\delta_i^2}}$, $\mathcal{Q}(-x) = 1 - \mathcal{Q}(x)$.

Integrating both sides of (29) with respect to z_k , we can obtain

$$\begin{aligned} P(z_i \geq 0 | u_i = +1) &= \int_0^\infty f(z_i | u_i = +1) dz_i \\ &= \frac{C^2 \delta_i^3}{\sqrt{2\pi}} \int_0^\infty \left[\exp\left(-\frac{z_i^2}{2\delta_i^2}\right) + \frac{\sqrt{2\pi}}{\delta_i \sqrt{1+\delta_i^2}} z_i \exp\left(-\frac{z_i^2}{2(1+\delta_i^2)}\right) \mathcal{Q}\left(-\frac{z_i}{\delta_i \sqrt{1+\delta_i^2}}\right) \right] dz_i \\ &= \frac{\delta_i}{\sqrt{2\pi}(1+\delta_i^2)} \left[\frac{\sqrt{2\pi}\delta_i}{2} + \frac{\sqrt{2\pi}\sqrt{1+\delta_i^2}}{2\delta_i} + \frac{\sqrt{2\pi}}{2\delta_i} \right] \\ &= \frac{1}{2} + \frac{1}{2\sqrt{1+\delta_i^2}} = \frac{1}{2} \left(1 + \sqrt{\frac{\gamma_i}{2+\gamma_i}}\right) \end{aligned} \quad (30)$$

193 where γ_i denotes the SNR of the Rayleigh fading reporting channel.

A similar analysis can be conducted for the case of $u_i = -1$, we have

$$f(z_i | u_i = -1) = \frac{C^2 \delta_i^3}{\sqrt{2\pi}} \exp\left(-\frac{z_i^2}{2\delta_i^2}\right) \left[1 - \sqrt{2\pi} C z_i \exp\left(\frac{C^2 z_i^2}{2}\right) \mathcal{Q}(C z_i)\right] \quad (31)$$

$$P(z_i \geq 0 | u_i = -1) = \int_0^\infty f(z_i | u_i = -1) dz_i = \frac{1}{2} \left(1 - \sqrt{\frac{\gamma_i}{2+\gamma_i}}\right) \quad (32)$$

By substituting (30) and (32) in (22) and (23), and after some simplified calculations, we can obtain the equivalent local probability of false alarm and detection as

$$P_{Fi} = P(z_i \geq 0 | \mathcal{H}_0) = \frac{1}{2} + \left(P_{fi} - \frac{1}{2} \right) \sqrt{\frac{\gamma_i}{2 + \gamma_i}} \quad (33)$$

$$P_{Di} = P(z_i \geq 0 | \mathcal{H}_1) = \frac{1}{2} + \left(P_{di} - \frac{1}{2} \right) \sqrt{\frac{\gamma_i}{2 + \gamma_i}} \quad (34)$$

and

$$P_{Mi} = 1 - P_{Di} = \frac{1}{2} + \left(P_{mi} - \frac{1}{2} \right) \sqrt{\frac{\gamma_i}{2 + \gamma_i}} \quad (35)$$

194 From (33) and (34), we can see that, if $P_{di} > \frac{1}{2}$, then $P_{Di} < P_{di}$. Only when $P_{di} < \frac{1}{2}$, then $P_{Di} > P_{di}$.
 195 In other words, the equivalent probability of miss detection at the FC high above the local probability
 196 of miss detection at each SUV. In the same manner, when $P_{fi} > \frac{1}{2}$, $P_{Fi} < P_{fi}$. Only when $P_{fi} < \frac{1}{2}$, the
 197 channel error "increases" P_{Fi} to be higher than P_{fi} . Without doubt, this is achieved with an accompanied
 198 rise in the probability of miss detection.

199 Besides, we also see that, as the reporting channel becomes more unreliable (low SNR situation,
 200 i.e., SNR $\gamma_i \rightarrow -\infty$), the equivalent probability P_{Di} (P_{Fi}) is close to $\frac{1}{2}$. As SNR $\gamma_i \rightarrow \infty$, P_{Di} (P_{Fi})
 201 comes near to P_{di} (P_{fi}), I would like to say this is a perfect reporting channel.

202 4.2. Global Probability of False Alarm and Miss Detection

203 Assuming that the reporting channels do not interfere with each other, and the delay is negligible.
 204 Once the fusion center decodes $\{z_i = g_i u_i + w_i; i = 1, 2, \dots, N\}$ and gets $\{v_i; i = 1, 2, \dots, N\}$, a global
 205 test statistic based on the counting rule is calculated linearly as follows:

$$\Lambda = \sum_{i=1}^N v_i \begin{cases} \geq T & \mathcal{H}_1 \\ < T & \mathcal{H}_0 \end{cases} \quad (36)$$

206 where T is the global decision threshold of counting rule, which can be in the form of $T = \alpha N$. This
 207 means that T or more SVUs decide hypothesis \mathcal{H}_1 , then the global decision is \mathcal{H}_1

208 From the preceding analysis, we can see that v_i is a binary random variable which follows a
 209 Bernoulli distribution characterized by the associated P_{Fi} and P_{Di} . It is noteworthy that the pairs
 210 (P_{Fi}, P_{Di}) of different SVUs are not really the same because the pairs (P_{fi}, P_{di}) or γ_i are different. So
 211 $\{v_i, i = 1, 2, \dots, N\}$ is a set of independent and non-identically distributed random variables. In
 212 consequence, their sum $\Lambda = \sum_{i=1}^N v_i$ will not approach the Binomial distribution any more. This makes
 213 the theoretical analysis and evaluation of \bar{Q}_m more sophisticated since it is indeed arduous to obtain a
 214 closed-form expression for such a distribution. Therefore, instead of relying on the exact distribution
 215 of Λ , we exploit a large-sample gaussian approximation for the sum of independent but not identically
 216 distributed random variables, known as the Lindberg-Feller CLT [20].

217 **Theorem 1.** Lindberg-Feller Central Limit Theorem (LF-CLT)

Assume that $\{X_i, i = 1, 2, \dots, N\}$ is a set of independently and non-identically distributed random variables with mean $E[X_i] = \mu_i$ and variance $D[X_i] = \delta_i^2$. Further, assume that the two following regularity conditions are satisfied

$$D[X_i] > \beta_1 \quad (37)$$

and

$$\mathbb{E} \left[|X_i - \mathbb{E}[X_i]|^3 \right] < \beta_2 \quad (38)$$

where β_1 and β_2 are positive values. Then, for sufficiently big N , $\sum_{i=1}^N X_i$ converges asymptotically to a Gaussian distribution characterized by

$$\sum_{i=1}^N X_i \rightarrow \mathcal{N} \left(\sum_{i=1}^N \mu_i, \sum_{i=1}^N \delta_i^2 \right) \quad (39)$$

218 For the applicability of LF-CLT, we will show how above-mentioned Lindberg-Feller conditions
 219 are satisfied in the Appendix. Consequently, in a large cognitive vehicular network, the LF-CLT can be
 220 used to approximately describe the distribution of the global decision statistic under both hypothesis
 221 \mathcal{H}_0 and \mathcal{H}_1 .

Because $\{v_i, i = 1, 2, \dots, N\}$ are all independent of each other, when N is sufficient large, in light of the LF-CLT [20], Λ is asymptotically Gaussian distributed with mean

$$\mu = \mathbb{E}\{\Lambda\} = \sum_{i=1}^N \mathbb{E}\{v_i\} = \begin{cases} \sum_{i=1}^N P_{Fi} & \mathcal{H}_0 \\ \sum_{i=1}^N P_{Di} & \mathcal{H}_1 \end{cases} \quad (40)$$

and variance

$$\sigma^2 = \mathbb{D}\{\Lambda\} = \sum_{i=1}^N \mathbb{D}\{v_i\} = \begin{cases} \sum_{i=1}^N P_{Fi}(1 - P_{Fi}) & \mathcal{H}_0 \\ \sum_{i=1}^N P_{Di}(1 - P_{Di}) & \mathcal{H}_1 \end{cases} \quad (41)$$

Consequently, the global probability of false alarm and miss detection at the FC in this case can be described by

$$Q_f = \mathcal{Q} \left(\frac{T - \bar{\mu}}{\sqrt{\sigma^2}} \right) = \mathcal{Q} \left(\frac{T - \sum_{i=1}^N P_{Fi}}{\sqrt{\sum_{i=1}^N P_{Fi}(1 - P_{Fi})}} \right) \quad (42)$$

$$Q_m = \mathcal{Q} \left(\frac{\bar{\mu} - T}{\sqrt{\sigma^2}} \right) = \mathcal{Q} \left(\frac{\sum_{i=1}^N P_{Di} - T}{\sqrt{\sum_{i=1}^N P_{Di}(1 - P_{Di})}} \right) \quad (43)$$

When the prior probabilities of presence and absence of PU are equal, i.e., $P(\mathcal{H}_1) = P(\mathcal{H}_0) = \frac{1}{2}$, the total probability of error detection can be written as

$$\begin{aligned} Q_e &= Q_f + Q_m \\ &= \mathcal{Q} \left(\frac{T - \sum_{i=1}^N P_{Fi}}{\sum_{i=1}^N P_{Fi}(1 - P_{Fi})} \right) + \mathcal{Q} \left(\frac{\sum_{i=1}^N P_{Di} - T}{\sum_{i=1}^N P_{Di}(1 - P_{Di})} \right) \end{aligned} \quad (44)$$

222 5. Numerical and Simulation Results

223 In this section, both theoretical and simulated results are provided to illustrate spectrum sensing
 224 performance in cognitive vehicular networks. The PU signal is assumed to enjoy unit power and
 225 be any kind of modulated signal with carrier frequency of 900Mhz and bandwidth of 6MHz. The
 226 sampling frequency in energy detector is equal to the bandwidth of PU signals, at the same time, the
 227 number of sampling observations during a sensing interval is $L = 50$. For all simulation cases, the
 228 average SNR is assumed to be the same for all SVUs, e.g., $\eta_0 = -8$ dB and $\gamma_0 = 5.5$ dB. The performances
 229 with respect to the local (global) probability of miss detection is estimated to meet the constraint on the

230 local (global) probability of false alarm of $P_f (Q_f) = 0.1$. The number of realizations made to compute
 231 the simulating probability of miss detection is 10000, which are set to guarantee the simulation results
 232 can validate the theoretic analysis in the low probability region.

233 Firstly, we manifest the performance of spectrum sensing with energy detector in non-cooperative
 234 cases, which is a key springboard of the study in cooperative cases. In Fig. 4, we provide the curves
 235 of the local sensing performance based on energy detection as a function of Doppler shift $F_d T_s$. With
 236 the carrier frequency and the sampling interval fixed, $F_d T_s$ value goes up as the vehicle velocity v .
 237 It is illustrated that the probability of miss detection declines with the increase of vehicle velocity.
 238 This reason is that high mobility gives us an opportunity to achieve more received signal information,
 239 thereby enables SVUs to obtain higher sensing performance.

240 In Fig. 5, we present the average \bar{P}_m curves as a function of the average SNR of sensing channels.
 241 The capability of energy detector declines quickly with the reduce of the average received SNR from
 242 10dB to -12dB. It can be seen that the simulating results are in accordance with the theoretical analysis
 243 for both \mathcal{M}_1 and \mathcal{M}_3 , justifying the validity of the analysis. The figure indicates that the expression
 244 (17) and (11) (18) give the corresponding upper and lower bounds of the average \bar{P}_m for spectrum
 245 sensing with energy detector under correlated Rayleigh fading channel.

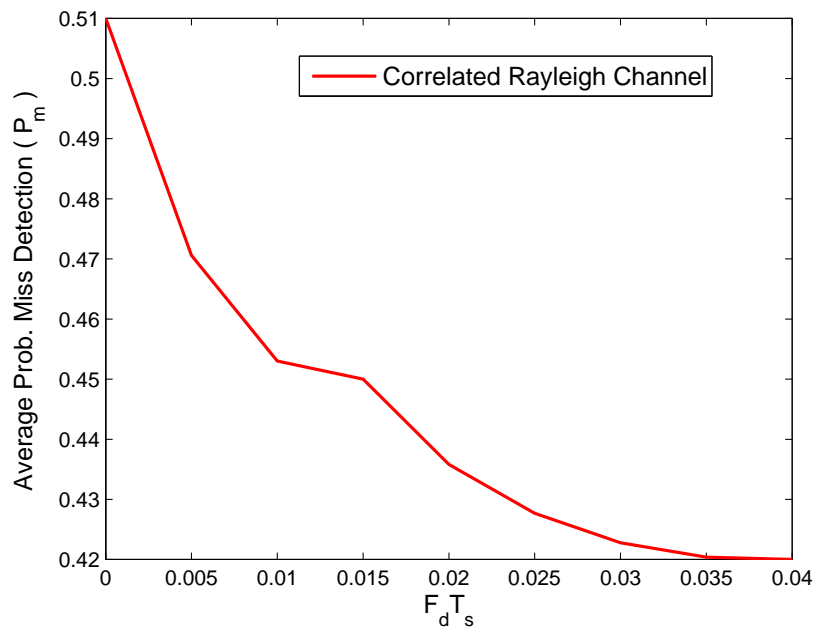


Figure 4. The local probability of miss detection for various $F_d T_s$.

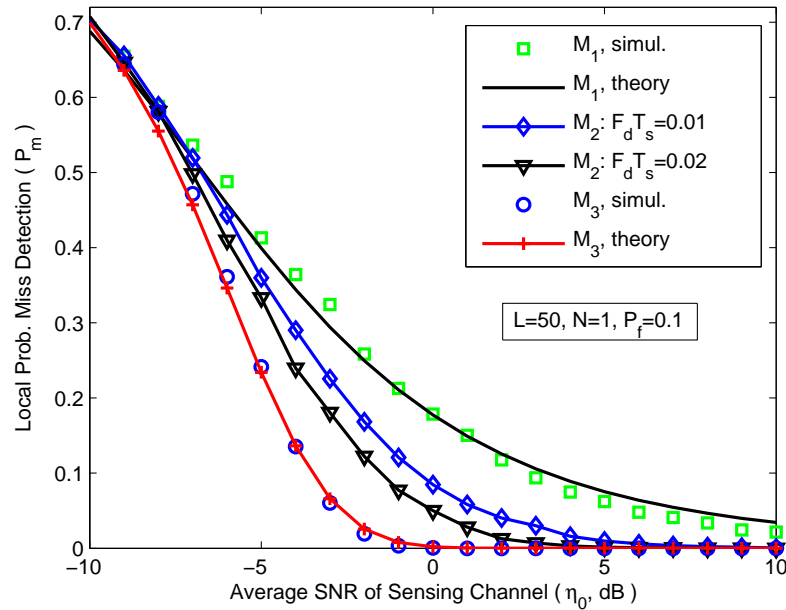


Figure 5. The local probability of miss detection for various average SNR of sensing channels.

246 Secondly, we focus on cooperative cases. In Fig. 6, we plot the global probability of miss detection
 247 (Q_m) as a function of the number of SUVs for hard fusion based on counting rule. As expected, the
 248 sensing performance shows an upward trend along with the increase of the number of SUVs. When N
 249 is extremely big, the global mis-detection probability approaches 0. For hard fusion, the Fig. 6 clearly
 250 demonstrate that the derived probability of miss detection based on Lindberg-Feller approximation is
 251 relatively poorer for a smaller number of SVUs. However, along with an increasing number of SVUs,
 252 the approximation asymptotically grows closer and closer to the exact sensing performance.

253 In Fig. 7, we present the ROC curves for different channel model. Note that, in the case of \mathcal{M}_1 and
 254 \mathcal{M}_3 , we obtain the average mis-detection probability for local sensing, allowing for a much smoother
 255 global probability curve than the case of \mathcal{M}_2 .

256 In Fig. 8, we present the average Q_m curves as a function of the average SNR of reporting channels.
 257 In the condition of poor reporting SNR, large bit error occurs, which severely degrade the detection
 258 performance. We can clearly see that cooperative sensing performance improves quickly with the
 259 increase of the average SNR of reporting channel from -8dB to 8dB. Note that the sensing performance
 260 in AWGN channel is always better than in Reyleigh channel.

261 In Fig. 9, we plot the global probability of error detection (Q_e) as a function of the local false-alarm
 262 probability. We can clearly see that, under certain conditions, there is an minimum probability of error
 263 detection, and that can be achieved when the local probabilities of false-alarm and mis-detection are
 264 equal ($P_f = P_m$). In Fig. 10, we plot the minimum achievable probability of error detection (Q_e) as a
 265 function of the number of SUVs.

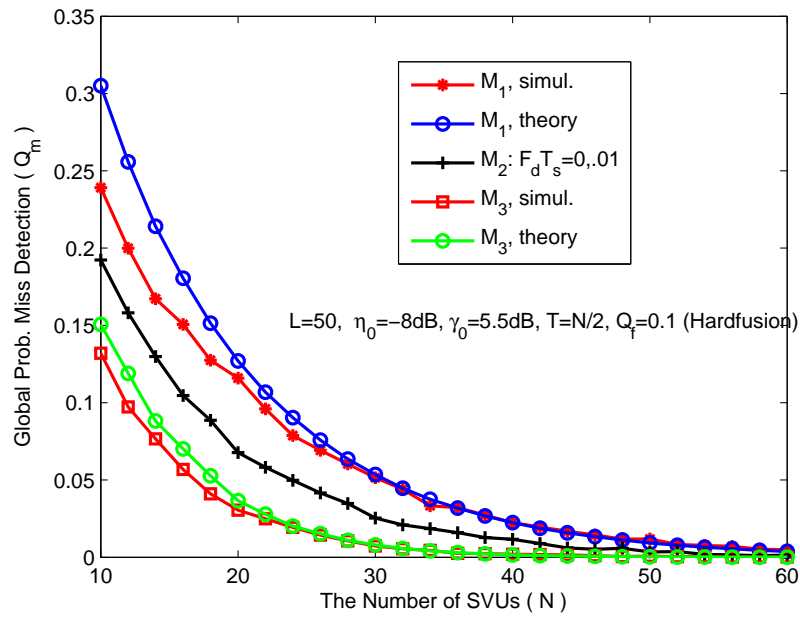


Figure 6. The global probability of miss detection for various number of SVUs.

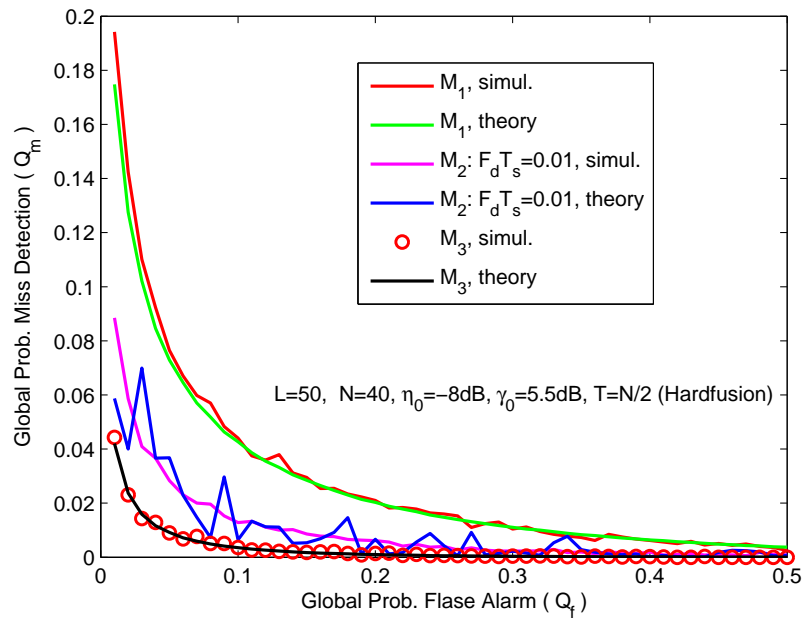


Figure 7. ROC curves for different channel model.

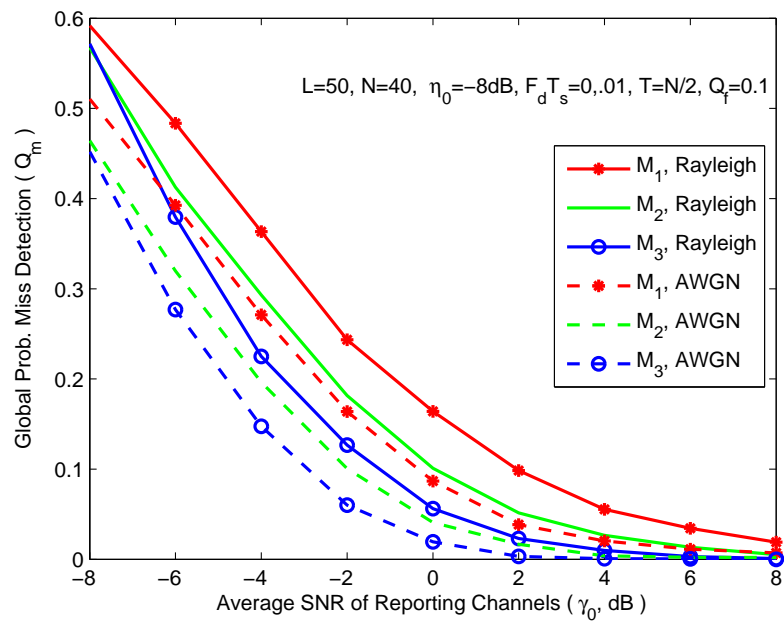


Figure 8. The global probability of miss detection for various average SNR of reporting channels.

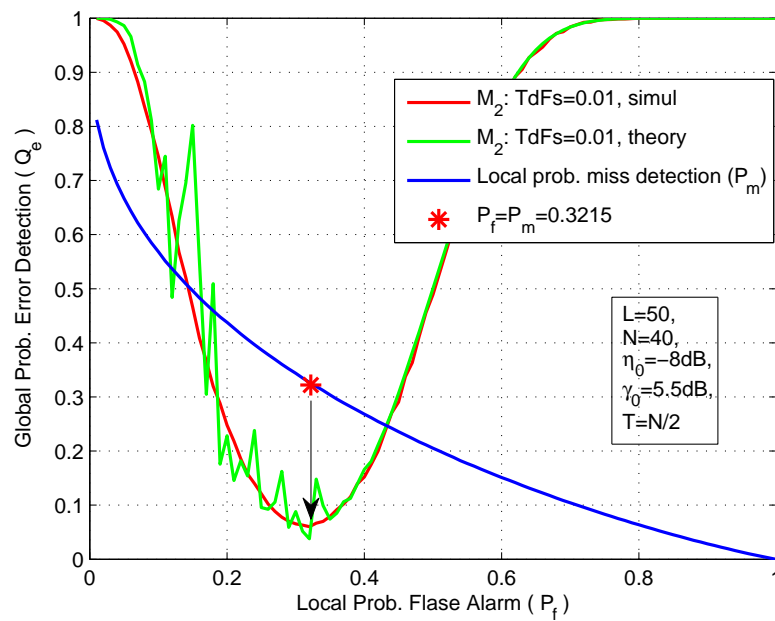


Figure 9. The global probability of error detection for various local probability of flase alarm.

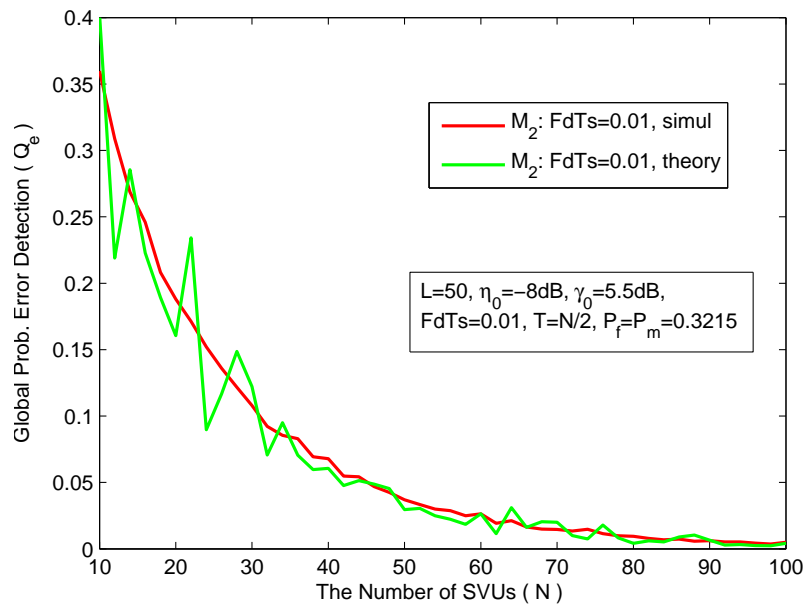


Figure 10. The global probability of error detection for various number of SVUs.

266 6. Conclusion

267 In this paper, we have researched the application of cognitive radio technique to vehicular
 268 environments for purpose of improving the reliability for vehicular communications. And for this,
 269 we evaluated the detection performance of spectrum sensing in mobile vehicular environments.
 270 Simulation results demonstrate that temporally correlation can not be neglected and be one of the
 271 considerable factors that may impact the sensing performance. In particular, highly mobility of the
 272 vehicles provides the opportunity to exploit temporal diversity at each vehicle. In spite of the fact that
 273 cooperative sensing have normally been considered as a viable means of producing better detection
 274 performance by making the most of spatial diversity among vehicles, we do believe that due to highly
 275 mobility, temporal diversity may be used in preference over vehicles' cooperation in the coming future.

276 **Acknowledgments:** This work was supported in part by the Key International Cooperation Project of Sichuan
 277 Province (2017HH0002), and in part by the NSFC under Grant 61601377 and Grant 61571373.

278 **Author Contributions:** Xiaomin Qian designed the system model, performed performance evaluations by
 279 theoretical analysis and simulation, and prepared the manuscript. Li Hao conceived the system model, carried out
 280 theoretical analysis and supervised the activities. Dadong Ni and Quang Thanh Tran discussed the main ideas
 281 and analyzed the results together. All authors approved the publication.

282 **Conflicts of Interest:** The authors declare no conflict of interest.

283 Appendix

284 In the following, we make clear how the two sufficient conditions (37) and (38) for the LF-CLT
 285 are satisfied for $\Lambda = \sum_{i=1}^N v_i$ under hypothesis \mathcal{H}_j , for $j = 0, 1$. Notice that in the LF-CLT, essentially,
 286 the objective of the two conditions is to ensure that no single random variable is dominate in its
 287 contribution to the summation operator.

In the first step we shall prove that the first condition is satisfied. As can be seen from (21) and (34), the variance of v_i , for $k = 1, 2, \dots, N$, under the hypotheses \mathcal{H}_1 can be represented as

$$\begin{aligned} D[v_i | \mathcal{H}_1] &= P_{Di} (1 - P_{Di}) \\ &= \left[\frac{1}{2} + \left(P_{di} - \frac{1}{2} \right) \sqrt{\frac{\gamma_i}{1 + \gamma_i}} \right] \left[\frac{1}{2} - \left(P_{di} - \frac{1}{2} \right) \sqrt{\frac{\gamma_i}{1 + \gamma_i}} \right] \\ &= \frac{1}{4} - \left(P_{di} - \frac{1}{2} \right)^2 \left(\frac{\gamma_i}{1 + \gamma_i} \right) \end{aligned} \quad (\text{A1})$$

288 It is sufficient to show that, under the hypothesis \mathcal{H}_1 , the variance of v_i is lower bounded by a
289 positive value, as long as the P_{di} are bounded away from 0 and 1.

In the next step, we show that the second condition (38) is satisfied. Let us make use of the fact that v_i is a binary random variable which follows a Bernoulli distribution characterized by the associated P_{Fi} and P_{Di} . It is plain enough that under the hypotheses \mathcal{H}_1

$$\begin{aligned} \mathbb{E} \left[|v_i - \mathbb{E}[v_i]|^3 | \mathcal{H}_1 \right] &= P_{Di} (1 - P_{Di}) \left(P_{Di}^2 + (1 - P_{Di})^2 \right) \\ &< P_{Di} (1 - P_{Di}) \end{aligned} \quad (\text{A2})$$

290 Accordingly, it is straightforward to see that $P_{Di}(1 - P_{Di})$ is upper bounded by a positive value.

291 In the above analysis, we prove that the two sufficient conditions (37) and (38) in the LF-CLT are
292 satisfied under the assumption of hypothesis \mathcal{H}_1 explicitly, but the same proved method can be carried
293 out to demonstrate the effectiveness under the hypothesis \mathcal{H}_0 .

294 References

- 295 1. Mitola J.; Maguire, G. Q. Cognitive radio: Making software radios more personal. *IEEE Pers. Commun.* **1999**,
296 6, 13-18.
- 297 2. Haykin, S. Cognitive radio: Brain-empowered wireless communications. *IEEE J. Sel. Areas Commun.* **2005**,
298 23, 201-220.
- 299 3. Singh, K. D.; Rawat, P.; Bonnin, J. Cognitive radio for vehicular ad hoc networks (CR-VANETs): approaches
300 and challenges. *EURASIP J. wireless commun. net.* **2014**, 2014.1: 49.
- 301 4. Wang, X. Y.; Ho, P. H. A Novel Sensing Coordination Framework for CR-VANETs. *IEEE Trans. Veh. Technol.*
302 **2010**, 59, 1936-1948.
- 303 5. Ali, A.; Hamouda, W. Advances on Spectrum Sensing for Cognitive Radio Networks: Theory and
304 Applications. *IEEE Commun. surveys tut.* **2017**, 19, 1277-1304.
- 305 6. Cicho-, K.; Kliks, A.; Bogucka, H. Energy-efficient cooperative spectrum sensing: A survey. *IEEE Commun.*
306 *Surveys Tut.* **2016**, 18, 1861-1886.
- 307 7. Mumtaz, S.; Huq, K. M. S.; Ashraf, M. I.; Rodriguez, J.; Monteiro, V.; Politis, C. Cognitive Vehicular
308 Communication for 5G. *IEEE Commun. Maga.* **2015**, 53, 109-117.
- 309 8. Felice, M. D.; Chowdhury, K. R.; Bononi, L. Analyzing the potential of cooperative Cognitive Radio
310 technology on inter-vehicle communication. In Proceedings of the IFIP Wireless Days, Venice, Italy, 1-6, Oct.
311 2010.
- 312 9. Rasheed, H.; Rajatheva, N. Spectrum sensing for cognitive vehicular networks over composite fading. *Int. J.*
313 *Veh. Technol.*, **2011**, 2011, 1-9.
- 314 10. Liu, Y.; Xie, S.; Yu, R.; Zhang, Y.; Zhang, X.; Yuen, C. Exploiting temporal and spatial diversities for spectrum
315 sensing and access in cognitive vehicular net- works. *Wireless Commun. Mobile Comput.* **2015**, 15, 2079-2094.
- 316 11. Aygun, B.; Wyglinski, A. M. A Voting Based Distributed Cooperative Spectrum Sensing Strategy for
317 Connected Vehicles. *IEEE Trans. Veh. Technol.*, **2017**, 66, 5109-5121.
- 318 12. Chembe, C., Noor, R. M., Ahmedy, I., Oche, M., Kunda, D., Liu, C. H. "Spectrum sensing in cognitive
319 vehicular network: State-of-Art, challenges and open issues," *Computer Commun.* **2017**, 97, 15-30.
- 320 13. Rahaman, M. F.; Khan, M. Z. Low Complexity Optimal Hard Decision Fusion under Neyman-Pearson
321 Criterion. *IEEE Signal Process. Lett.* **2017**, 1, 1-5.

- 322 14. Chaudhari, S.; Lunden, J.; Koivunen, V.; Poor, H. V. Cooperative sensing with imperfect reporting channels:
323 Hard decisions or soft decisions? *IEEE Trans. Signal Process.* **2012**, *60*, 18-28.
- 324 15. Simon, M. K.; Alouini, M. *Digital communication over fading channels.*, Vol. 95, John Wiley & Sons, 2005.
- 325 16. Tsitsiklis, J. N. Decentralized detection. *Advances in Statistical Signal Processing*. Greenwich, CT: JAI, **1993**, *2*,
326 297-344.
- 327 17. Herath, S. P.; Rajatheva, N.; Tellambura, C. Energy detection of unknown signals in fading and diversity
328 reception. *IEEE Trans. Commun.*, **2011**, *59*, 2443-2453.
- 329 18. Atapattu, S.; Tellambura, C.; Jiang, H. Energy detection based cooperative spectrum sensing in cognitive
330 radio networks. *IEEE Trans. wireless commun.*, **2011**, *10*, 1232-1241.
- 331 19. Nuttall, A. H. *Some integrals involving the Q-function*. DTIC Document, Tech.Rep., 1972.
- 332 20. Peebles, P. Z.; Shi, B. E. *Probability, random variables, and random signal principles*. McGraw-Hill: New York,
333 USA, 2001.

334